Journal of Molecular and Cellular Cardiology 122 (2018) 34–46

Contents lists available at ScienceDirect

Journal of Molecular and Cellular Cardiology

journal homepage: www.elsevier.com/locate/yjmcc

Original article

Sympathoadrenergic suppression improves heart function by upregulating the ratio of sRAGE/RAGE in hypertension with metabolic syndrome

Simina-Ramona Selejan[a,*,1], Dominik Linz[a,1], Anna-Maria Tatu[a], Mathias Hohl[a], Thimoteus Speer[b], Sebastian Ewen[a], Felix Mahfoud[a], Ingrid Kindermann[a], Olesja Zamyatkin[a], Andrey Kazakov[a], Ulrich Laufs[a], Michael Böhm[a]

[a] Klinik für Innere Medizin III (Kardiologie, Angiologie und Internistische Intensivmedizin), Universität des Saarlandes, Homburg, Saar, Germany
[b] Klinik für Innere Medizin IV (Nieren- und Hochdruckkrankheiten), Universität des Saarlandes, Homburg, Saar, Germany

ARTICLE INFO

Keywords:
Receptor for advanced glycation end products
hypertension
metabolic syndrome
renal denervation
fibrosis
HMGB1 protein

ABSTRACT

Receptors-for-Advanced-Glycation-End-products (RAGE) activate pro-inflammatory programs mediated by carboxymethyllysine (CML) and high-mobility-group-box1 protein (HMGB1). The soluble isoform sRAGE neutralizes RAGE-ligands preventing cardiovascular complications in conditions associated with increased sympathetic activation like hypertension and diabetes. The effects of sympathetic modulation on RAGE/sRAGE-balance and end-organ damage in metabolic syndrome on top of hypertension remains unknown. We hypothesized that increased sympathoadrenergic activity might lead to an unfavourable RAGE/sRAGE regulation. Renal denervation (RDN) was used to modulate sympathetic activation in obese spontaneously hypertensive rats (SHRobRDN) versus sham-operated obese spontaneously hypertensive rats (SHRob), their hypertensive lean controls (SHR) and non-hypertensive controls. Cardiac fibrosis was assessed by histological analysis and sRAGE/RAGE and ligand levels by Western blotting. Levels of CML and HMGB1 were highest in SHRob and were significantly lowered by RDN in serum (−44% and −45%) and myocardium (−25% and −52%). Myocardial RAGE was increased in SHR (+72% versus controls) and in SHRob (+68% versus SHR) while sRAGE decreased (−50% in SHR versus controls and −51% in SHRob versus SHR). RDN reduced myocardial RAGE expression. (−20%) and increased sRAGE levels in heart (+80%) and serum (+180%) versus sham-operated SHRob. Myocardial fibrosis correlated inversely with myocardial sRAGE content ($r = -0.79$; $p = .004$; $n = 10$). Myocardial sRAGE shedding active A-Disintegrin-And-Metalloprotease-10 (ADAM-10) was decreased in SHR (−33% versus controls) and in SHRob (−54% versus SHR), and was restored after RDN (+129% versus SHRob). Serum ADAM-10 activity was also decreased in SHRob (−66% versus SHR) and restored after RDN (+150% versus SHRob). In vitro, isoproterenol induced a ß1-adrenergic receptor mediated increase of RAGE expression in splenocytes (+200%) and decreased sRAGE secretion of splenocytes and cardiac fibroblasts (−50% and −49%) by ß2-adrenergic receptor stimulation mediated suppression of ADAM-10 activity. In conclusion, sympathetic activity affects sRAGE/RAGE-balance, which can be suppressed through sympathetic modulation by RDN, preventing RAGE-induced cardiac damage in hypertension with metabolic syndrome.

1. Introduction

The multi-ligand receptor RAGE (Receptor-for-Advanced-Glycation-End-products) was initially described as the signal-transducing receptor for advanced glycation end products (AGEs) and is involved in microvascular complications and end-organ damage associated with increased sympathetic activation in hypertension, diabetes and heart failure [1–6]. The soluble form of RAGE (sRAGE) comprises only the RAGE ectodomain and acts as a ligand decoy, competitively inhibiting RAGE activation and oxidative stress [1, 6]. Endogenous soluble RAGE isoforms are circulating in plasma and tissues and are suspected to inversely reflect cellular RAGE activity [7], with most sRAGE being produced by ADAM-10 mediated RAGE cleavage [8–9]. Whether modulation of sympathetic activation is responsible for the observed changes in RAGE/sRAGE balance, however, is unknown. Renal sympathetic denervation (RDN) reduces afferent and efferent sympathetic

* Corresponding author at: Klinik für Innere Medizin III, Kirrbergerstr. 100, Geb. 41.1 (IMED), Universität des Saarlandes, D-66421 Homburg, Saar, Germany.
E-mail address: simina.selejan@uks.eu (S.-R. Selejan).
[1] S. Selejan and D. Linz contributed equally to this study.

https://doi.org/10.1016/j.yjmcc.2018.08.003
Received 18 February 2018; Received in revised form 16 July 2018; Accepted 5 August 2018
Available online 07 August 2018

Table 1
Metabolic parameters, left ventricular and renal function.

	Control	SHR	SHRob	SHRobRDN	Control Vs. SHR	SHR Vs. SHRob	SHRob Vs. SHRobRDN	Control Vs. SHRob RDN
	n = 5–6	n = 6–7	n = 5–6	n = 5–6				
Parameters					P-value			
Creatinine umol/l	21 ± 1.3	29 ± 0.9	32.3 ± 5.3	21.3 ± 7.3	0.062	0.437	0.038	0.958
GFR l/kg/h	0.6 ± 0.02	0.4 ± 0.02	0.2 ± 0.02	0.3 ± 0.07	< 0.001	< 0.001	0.019	< 0.001
EF (%)	66.0 ± 1.8	51.2 ± 1.2	45.7 ± 1.6	54.1 ± 1.2	< 0.001	0.041	0.007	< 0.001
LVedP mm Hg	4.7 ± 1.4	6.0 ± 2.7	16.1 ± 2.3	7.4 ± 2.2	0.703	0.012	0.051	0.494
RR (MAP) mm Hg	116 ± 2.9	199 ± 5.6	224 ± 5	179 ± 12.2	< 0.001	0.031	< 0.001	< 0.001
HR bpm	328 ± 1.3	305 ± 13.7	276 ± 9.6	277 ± 13.4	0.285	0.119	0.994	0.026
HW g	1.55 ± 0.05	1.64 ± 0.07	1.61 ± 0.06	1.66 ± 0.07	0.234	0.738	0.646	0.214
BW g	618 ± 8.4	419 ± 11	697 ± 20.2	632 ± 36.7	< 0.001	< 0.001	0.157	0.999
HW/100 g BW ratio	0.24 ± 0.004	0.39 ± 0.011	0.23 ± 0.016	0.27 ± 0.025	< 0.001	< 0.001	0.094	0.201
Insulin Pg/ml	854 ± 231	1157 ± 294	10,126 ± 1518	7714 ± 1289.3	0.809	< 0.001	0.118	< 0.001
Glucose mmol/l	5.0 ± 0.11	5.76 ± 0.17	5.99 ± 0.17	5.13 ± 0.37	0.055	0.571	0.038	0.569
HbA1C % (mmol/mol)	3.9% ± 0.01 (19 ± 0.05)	3.6% ± 0.04 (16 ± 0.18)	3.7% ± 0.1 (17 ± 0.46)	3.7% ± 0.14 (17 ± 0.64)	0.132	0.464	0.462	0.879
Renal Norepinephrine pg/mg	103.5 ± 14.7	98.2 ± 2.3	108.7 ± 8.9	10.9 ± 2.4	0.628	0.634	< 0.001	< 0.001

GFR: glomerular filtration rate.
EF: left-ventricular ejection fraction.
LVedP: left-ventricular end-diastolic pressure.
MAP: mean arterial pressure.
HR: heart rate.
HW: heart weight.
BW: body weight.

nerve activity and has been developed to lower blood pressure in patients with uncontrolled hypertension [10–12]. Experimental and observational data suggest additional effects beyond blood pressure lowering such as reduction in myocardial hypertrophy, improved glucose tolerance and amelioration of microalbuminuria [13–16]. We have recently characterized a rat model of metabolic syndrome with hypertension, the spontaneously hypertensive obese rat (SHRob) carrying an additional mutation in the leptin receptor [17, 18]. In addition to hypertension, SHRob express further abnormal phenotypes including obesity, hyperinsulinemia and hyperlipidemia, a moderate decrease in LV-systolic function and diastolic dysfunction [18]. The exact mechanisms of how metabolic syndrome on top of hypertension results in more pronounced end-organ damage are still unknown. However, sympathetic modulation by RDN in SHRob for example has led to an improvement in renal and cardiac function [19].

The present study aimed to investigate the effect of in-vivo modulation of sympathoadrenergic activity by RDN on the cardiac ligand-RAGE/sRAGE-axis and subsequent cardiac remodelling in a rat model of metabolic syndrome on top of hypertension. In order to control for blood-pressure confounding, β-adrenergic receptor mediated RAGE/sRAGE regulation was studied in isolated rat mononuclear cells (splenocytes) and cardiac fibroblasts.

2. Materials and methods

2.1. Animals

Male obese spontaneously hypertensive rats (SHRob), their heterozygous hypertensive control rats (lean SHR) and non-hypertensive non-obese control rats (Sprague Dawley; controls) were purchased from Charles River GmbH (Sulzfeld, Germany) at the age of 10 weeks. The animals were housed individually in standard cages and received standard chow (standard diet #1320, Altromin, Lage, Germany) and tap water ad libitum. RDN or sham-operation was performed in SHRob at the age of 32 weeks and rats were killed at the age of 45 weeks. For the isolation of primary rat cardiac fibroblasts, Sprague Dawley rats from Charles River GmbH (Sulzfeld, Germany) aged 52 weeks were sacrificed instantly under general deep anaesthesia. All animal studies were performed in accordance to the German law for the protection of animals. Furthermore, the investigation conforms with the guide for the Care and Use of laboratory Animals published by the US National Institutes of Health (NIH Publication No. 85-23, revised 1996). The study was approved by the regional commission in charge (Darmstadt, Germany).

2.2. Reagents

See online supplement.

2.3. Renal denervation

Renal denervation (RDN) was performed in SHRob at the age of 32 weeks (SHRobRDN) when metabolic syndrome was fully established to test the role of renal sympathetic innervation on the further progression of cardiac end-organ damage. The detailed procedure is described in the online supplements.

2.4. Metabolic cages, cardiac MRI and invasive functional measurements, sample asservation, histological analysis and immunoblotting

The protocols are described in detail in the online-only data supplement.

2.5. Isolation of primary rat cardiac fibroblasts and splenocytes, culture conditions, cell fractionation, protein and gene expression analyses

Detailed protocols are provided in the online supplements.

2.6. Statistics

Statistical analysis was performed with Graph Pad Prism (version 5.0; GraphPad Software, San Diego California, USA). Results are presented as means ± SEM. Significance was estimated with two-way-ANOVA with Fisher-LSD post hoc test for multiple comparisons. Normal contribution of data was tested by Kolmogorov-Smirnov and Lilliefors test and Spearman's or Pearson's correlations are shown respectively. A value of $p < .05$ was considered significant.

3. Results

3.1. Effects of renal denervation on renal and metabolic parameters

Metabolic parameters are summarized in Table 1. A reduction in renal norepinephrine tissue content was observed in RDN-treated SHRob rats (SHRobRDN) at 3 months after the procedure as compared to sham-operated SHRob pointing out to a successful sympathetic denervation of the kidneys (Table 1; 108.7 ± 8.9 pg/ml in SHRob vs. 10.9 ± 2.4 pg/ml in SHRobRDN, $p < .001$). Renal function as depicted by GFR was markedly reduced in SHRob as compared to SHR and normotensive controls (SHRob 0.2 ± 0.02 l/kg/h versus SHR

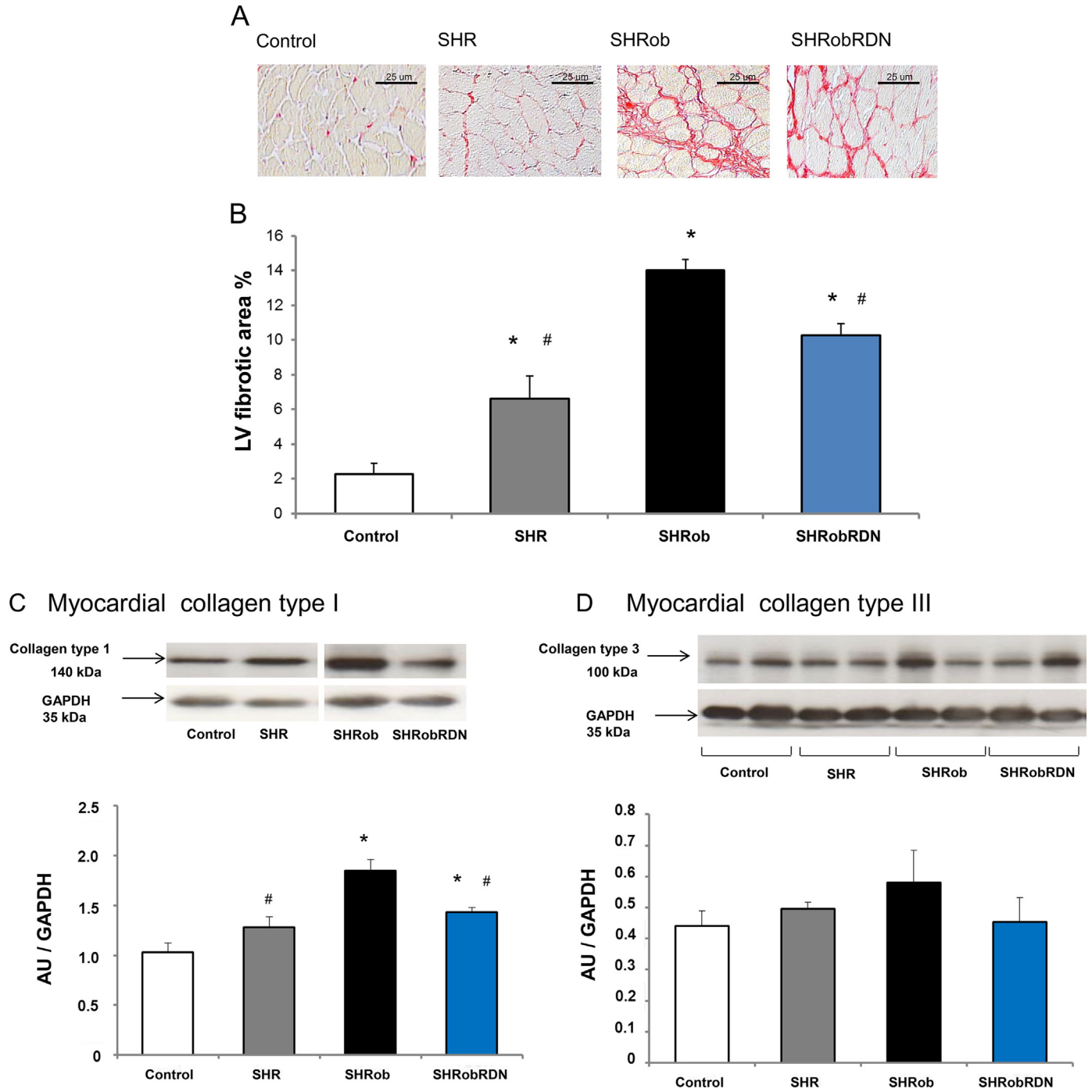

Fig. 1. A) Representative histological pictures (picrosirius red staining) and B) Quantification of left ventricular fibrotic area (interstitial fibrillar collagen fractional area (%)) in normotensive controls (n = 5), SHR (n = 6), SHRob (n = 5) and SHRobRDN (n = 5). C) Representative Western blot of myocardial collagen type I (upper panel; images from different parts of the same gel) and quantification of collagen type I (lower panel) in normotensive controls (n = 5), SHR (n = 6), SHRob (n = 5) and SHRobRDN (n = 5). Collagen type I in arbitrary units (AU) normalized to GAPDH. D) Representative Western blot of myocardial collagen type III (upper panel) and quantification of collagen type III (lower panel) in normotensive controls (n = 5), SHR (n = 6), SHRob (n = 5) and SHRobRDN (n = 5). Collagen type III in arbitrary units (AU) normalized to GAPDH. *$p < .05$ versus Control; #$p < .05$ versus SHRob. E) Representative Western blot (upper panel) and quantification of collagen type I secretion in supernatants of rat cardiac fibroblasts repeatedly stimulated with isoproterenol (ISO) 0.1 umol/l (n = 4) in the presence or absence of CGP (ß1-selective antagonist; 0.3 umol/l) or ICI (ß2-selective antagonist; 0.1 umol/l) for 72 h every 24 h. *$p < .05$ versus Control and ISO + CGP; #$p < .05$ versus ISO + CGP. (For interpretation of the references to colour in this figure legend, the reader is referred to the web version of this article.)

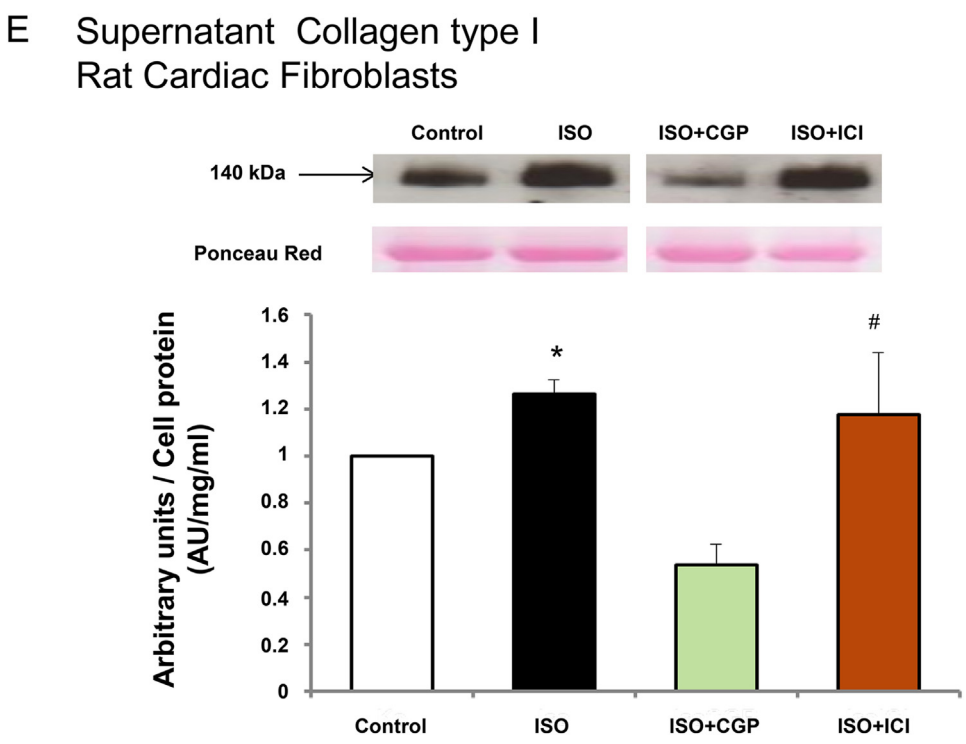

Fig. 1. (*continued*)

Table 2
Interstitial fibrosis, myocardial and serum RAGE/sRAGE, and RAGE-ligand levels (CML and HMGB1) and inflammatory cytokines.

	Control	SHR	SHRob	SHRobRDN	Control vs. SHR	SHR vs. SHRob	SHRob vs. SHRobRDN	Control vs. SHRobRDN
	n = 5–6	n = 6–7	n = 5–6	n = 5–6				
Parameters					p-value			
Myocardial fibrosis %	2.3 ± 0.6	6.6 ± 1.3	13.3 ± 0.7	10.3 ± 0.7	0.008	< 0.001	0.041	< 0.001
Myocardial sRAGE AU/GAPDH	2.6 ± 0.2	1.3 ± 0.2	0.6 ± 0.1	1.2 ± 0.1	0.005	0.042	0.043	0.006
Myocardial RAGE AU/GAPDH	1.6 ± 0.2	2.7 ± 0.5	4.5 ± 0.2	3.4 ± 0.6	0.044	0.003	0.066	0.003
Serum sRAGE AU/mg/ml serum protein	11.4 ± 5.0	15.4 ± 2.7	4.9 ± 1.7	13.9 ± 2.9	0.265	0.008	0.033	0.558
Myocardial CML AU/GAPDH	12.1 ± 1.2	16.5 ± 1.4	19.2 ± 1.2	14.4 ± 0.8	0.015	0.156	0.017	0.171
Serum CML AU/mg/ml serum protein	12.7 ± 0.9	19.3 ± 2.5	18.0 ± 1.4	10.0 ± 1.3	0.012	0.565	0.001	0.194
Myocardial HMGB1 AU/GAPDH	1.5 ± 0.2	1.5 ± 0.3	3.5 ± 0.6	1.7 ± 0.4	0.817	0.003	0.022	0.545
Serum HMGB1 AU/mg/ml serum protein	4.6 ± 0.3	5.7 ± 0.5	8.8 ± 1.8	4.9 ± 0.5	0.386	0.035	0.026	0.793
Collagen type I AU/GAPDH	1.03 ± 0.09	1.28 ± 0.11	1.85 ± 0.11	1.43 ± 0.05	0.123	< 0.001	0.008	0.022
Collagen type III AU/GAPDH	0.44 ± 0.05	0.5 ± 0.02	0.58 ± 0.1	0.45 ± 0.08	0.614	0.409	0.219	0.910
TGFß AU/GAPDH	0.23 ± 0.07	0.25 ± 0.09	0.16 ± 0.04	0.18 ± 0.02	0.799	0.271	0.876	0.497
CTGF AU/GAPDH	0.26 ± 0.16	0.41 ± 0.07	0.45 ± 0.13	0.31 ± 0.08	0.323	0.816	0.349	0.758
Myocardial esRAGE AU/GAPDH	0.18 ± 0.02	0.18 ± 0.01	0.23 ± 0.01	0.21 ± 0.01	0.909	0.031	0.407	0.171
Serum esRAGE AU/mg/ml serum protein	39.34 ± 6.71	46 ± 5.05	33.35 ± 5.52	38.11 ± 5.56	0.337	0.068	0.522	0.888
Myocardial Active ADAM-10 AU/GAPDH	13.06 ± 0.97	8.71 ± 0.64	3.97 ± 0.48	9.08 ± 1.24	0.015	0.005	0.003	0.024
Serum active ADAM-10 AU/mg/ml serum protein	52.74 ± 5.02	36.97 ± 7.94	12.7 ± 2.8	31.83 ± 5.62	0.102	0.015	0.028	0.079
TNFalpha AU/GAPDH	2.02 ± 0.14	1.96 ± 0.16	1.6 ± 0.19	1.12 ± 0.19	0.828	0.165	0.083	0.006
IL-6 AU/GAPDH	1.1 ± 0.09	1.25 ± 0.03	1.34 ± 0.13	0.59 ± 0.12	0.283	0.592	0.001	0.012

AU: arbitrary units.
sRAGE: soluble receptor for advanced glycation end products.
esRAGE:endogenous secretory RAGE.
CML: carboxymethyllysine.
HMGB1: high mobility group box1 protein.
GAPDH: Glyceraldehyde 3-phosphate dehydrogenase.
TGFß: Transforming Growth Factor ß.
CTGF: Connective Tissue Growth Factor.
ADAM-10: A Disintegrin And Metalloprotease − 10.
TNFα: Tumor Necrosis Factor α.
IL-6: Interleukine 6.

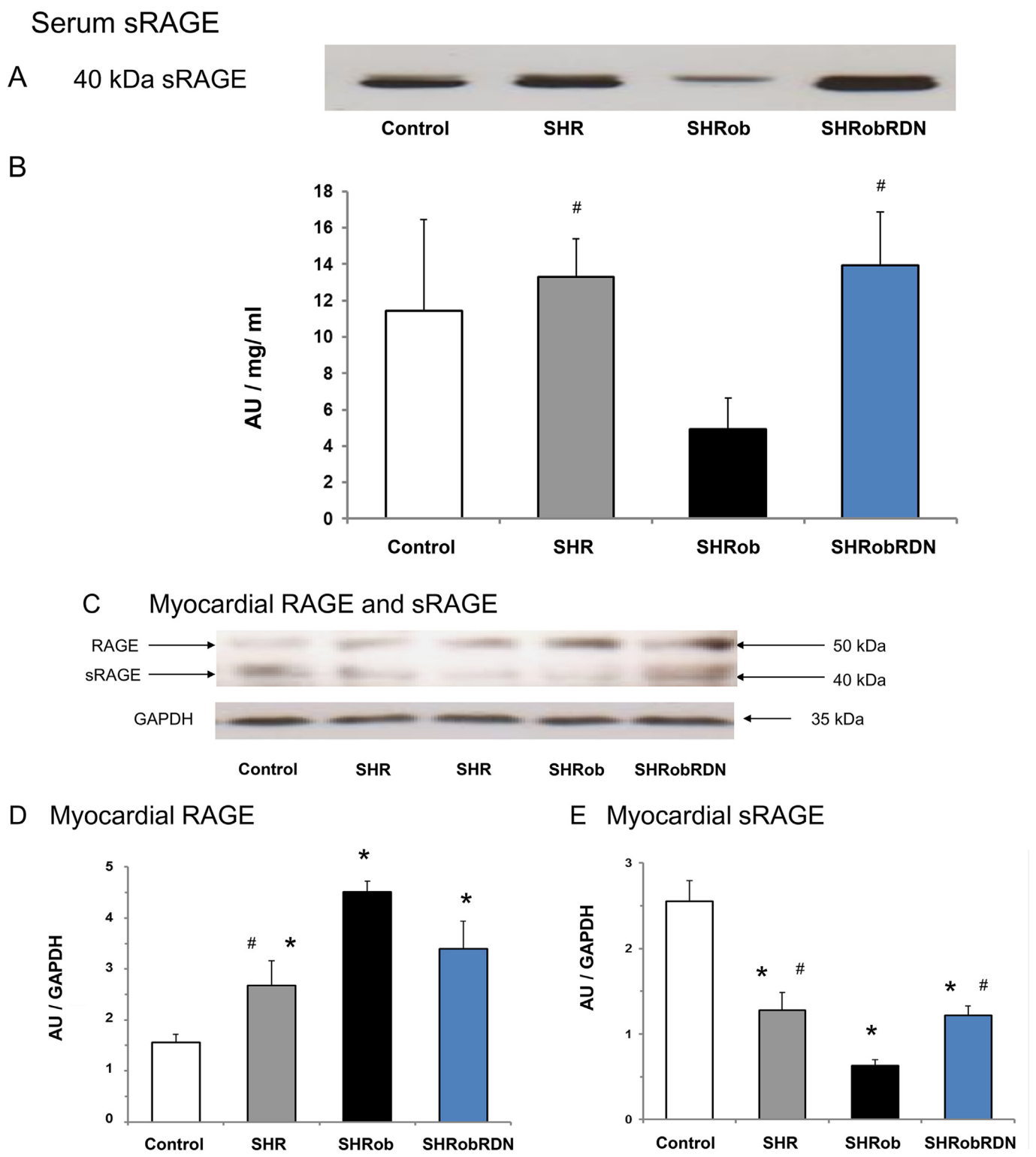

Fig. 2. A) Representative Western blot and B) Quantification of sRAGE in serum samples from normotensive controls (n = 5), SHR (n = 6), SHRob (n = 5) and SHRobRDN (n = 5). sRAGE in arbitrary units (AU) normalized to serum protein concentration. C) Representative Western blot and D) Quantification of myocardial RAGE and E) myocardial sRAGE in myocardial homogenates from normotensive controls (n = 5), SHR (n = 6), SHRob (n = 5) and SHRobRDN (n = 5). RAGE and sRAGE in arbitrary units (AU) normalized to GAPDH. F) Representative Western blot (upper panel; images from different parts of the same gel) and quantification of active ADAM-10 (lower panel) in serum samples from normotensive controls (n = 5), SHR (n = 6), SHRob (n = 5) and SHRobRDN (n = 5). Active ADAM-10 in arbitrary units (AU) normalized to serum protein concentration. G) Representative Western blot (upper panel; images from different parts of the same gel) and quantification of myocardial active ADAM-10 (lower panel) in homogenates from normotensive controls (n = 5), SHR (n = 6), SHRob (n = 5) and SHRobRDN (n = 5). Active ADAM-10 in arbitrary units (AU) normalized to GAPDH. *p < .05 versus Control; #p < .05 versus SHRob.

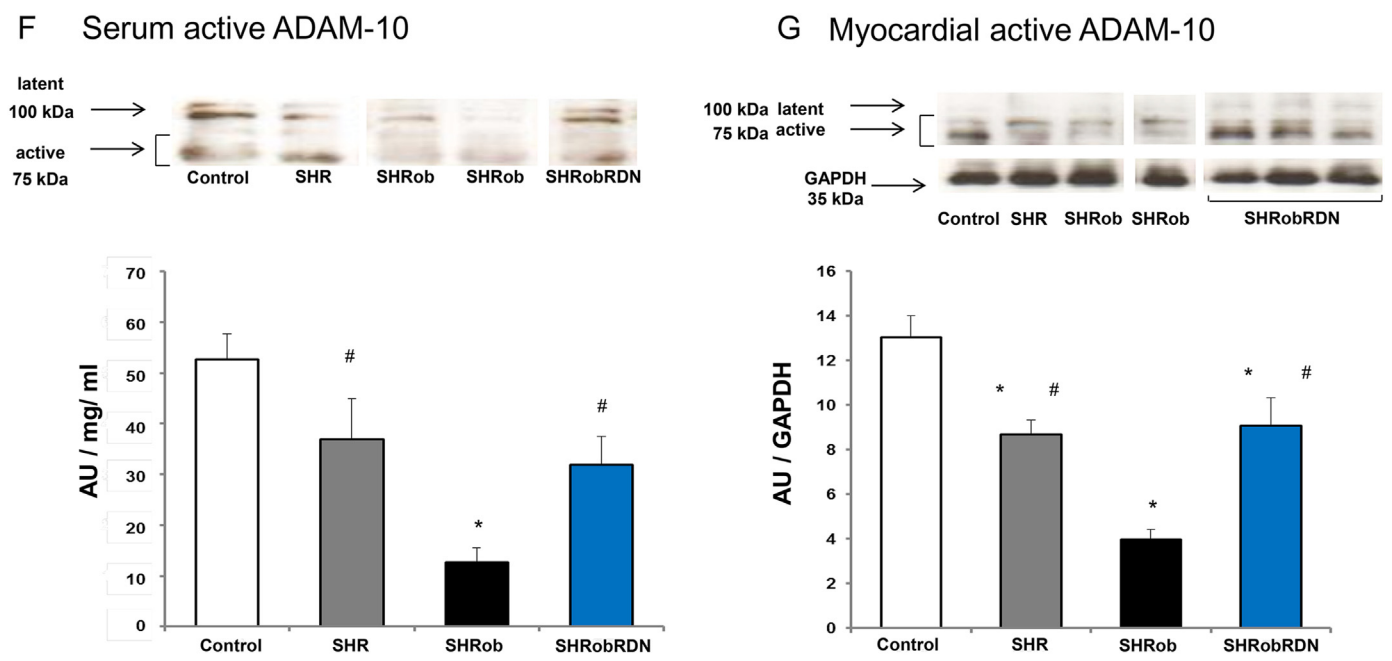

Fig. 2. (*continued*)

0.4 ± 0.02 and controls 0.6 ± 0.02, p < .001 for each comparison), but was significantly improved after RDN (0.3 ± 0.07 l/kg/h, p = .019 versus SHRob). Also, creatinine levels decreased after RDN (SHRob 32.3 ± 5.3 umol/l versus SHRobRDN 21.3 ± 7.3 µmol/l; p = .038). Fasting insulin levels were significantly increased in SHRob compared with their lean hypertensive littermates and to normotensive controls (SHRob 10,126 ± 1518 pg/ml versus SHR 1157 ± 294 pg/ml and controls 854 ± 231 pg/ml, p < .001 for each comparison) and showed a trend towards improvement after RDN, however without reaching statistical significance (Table 1). As the SHRob phenotype does not yet display overt diabetes, HbA1C data were similar in all four groups (Table 1).

3.2. Effects of renal denervation on cardio-functional parameters

Averaged values of the MRI-derived and invasively measured cardiac functional parameters are summarized in Table 1. LV-ejection fraction as determined by cardiac magnetic resonance imaging was slightly reduced in SHRob compared with SHR and controls (45.7 ± 1.6% in SHRob vs. 51.2 ± 1.2% in SHR, p = .041, and 66 ± 1.8% in controls, p < .001 versus SHRob) and was significantly improved after RDN (SHRobRDN 54.1 ± 1.2%, p = .007 versus SHRob). Left-ventricular end-diastolic pressure (LVedP) as determined by invasive measurement procedures was markedly increased in SHRob compared to lean littermates or normotensive controls and was reduced after RDN (Table 1). Mean arterial pressure was significantly increased in SHR and SHRob as compared with controls (Table 1) and was reduced after RDN (179 ± 12 mm Hg in SHRobRDN vs.224 ± 5 mmHg in SHRob, p < .001).

3.3. Effect of renal denervation on myocardial fibrosis

Interstitial collagen deposition, as determined by Sirius Red Staining (Fig. 1A), was significantly increased in SHR compared to normotensive controls (Table 2, Fig. 1B; 6.6 ± 1.3% in SHR versus 2.3 ± 0.6% in controls, p = .008) and further increased in SHRob compared to SHR (13.3 ± 0.7% in SHRob versus 6.6 ± 1.3% in SHR, p < .001), but was attenuated by RDN (10.3 ± 0.7% in SHRobRDN; p = .041 versus SHRob). Differential analysis of collagen types I and III showed a numerical increase in collagen I content in SHR compared to controls (Table 2, Fig. 1C; 1.28 ± 0.11 AU/GAPDH in SHR versus 1.03 ± 0.09 in controls, p = .123) and a significant increase in SHRob compared to SHR (1.85 ± 0.11 AU/GAPDH in SHRob versus 1.28 ± 0.11 in SHR, p < .001). Collagen type I expression was reduced by RDN (1.43 ± 0.05 AU/GAPDH in SHRobRDN, p = .008 versus SHRob). Collagen type III showed no differences between the groups (Table 2, Fig. 1D). In vitro stimulation of rat cardiac myocytes with isoproterenol augmented secretion of collagen type I into the supernatant, which could be prevented by selective ß1-AR-blockade (Fig. 1E).

Expression analyses of the pro-fibrogenic factors TGFß (Transforming Growth Factor ß) and CTGF (Connective Tissue Growth Factor) in rat myocardial samples showed no significant differences between the groups (Table 2, Supplemental Figs. 1A und 2A), neither could TGFß or CTGF secretion be induced in vitro by isoproterenol treatment of cardiac fibroblasts or splenocytes (Supplemental Figs. 1B–C and 2B–C).

3.4. Renal denervation increases circulating serum sRAGE levels and myocardial sRAGE

Serum sRAGE levels as assessed by Western blot analysis (Table 2, Fig. 2A) were significantly decreased in SHRob as compared to lean SHR (Fig. 2B; 4.9 ± 1.7 AU/mg/ml in SHRob versus 15.4 ± 2.7 in SHR, p = .008) and were significantly augmented after RDN (13.9 ± 2.9 AU/mg/ml in SHRobRDN, p = .033 versus SHRob).

Myocardial RAGE (Table 2, Fig. 2C and D) was markedly increased in SHRob as compared to SHR and to normotensive controls (4.5 ± 0.2 AU/GAPDH in SHRob versus 2.7 ± 0.5 AU/GAPDH in SHR and 1.6 ± 0.2 AU/GAPDH in controls; p < .003 for each comparison) (Table 2, Fig. 2D). RDN did not significantly affect myocardial content of full-length RAGE, although it showed a trend towards RAGE-down-regulation in the SHRobRDN group (Table 2, Fig. 2D). sRAGE myocardial content (Fig. 2E) on the other hand was significantly decreased in SHRob as compared to SHR and controls (Table 2, Fig. 2E; 0.6 ± 0.1 AU/GAPDH in SHRob versus 1.3 ± 0.2 AU/GAPDH in SHR versus 2.6 ± 0.2 AU/GAPDH in controls; p = .0001–0.02 for each comparison) while in SHRobRDN sRAGE levels were significantly improved (1.2 ± 0.1 AU/GAPDH, p = .043 versus SHRob). Myocardial sRAGE expression showed a strong negative correlation with LV-fibrosis data (Supplemental Fig. 3; r = −0.79, p = .004, n = 10 SHRob

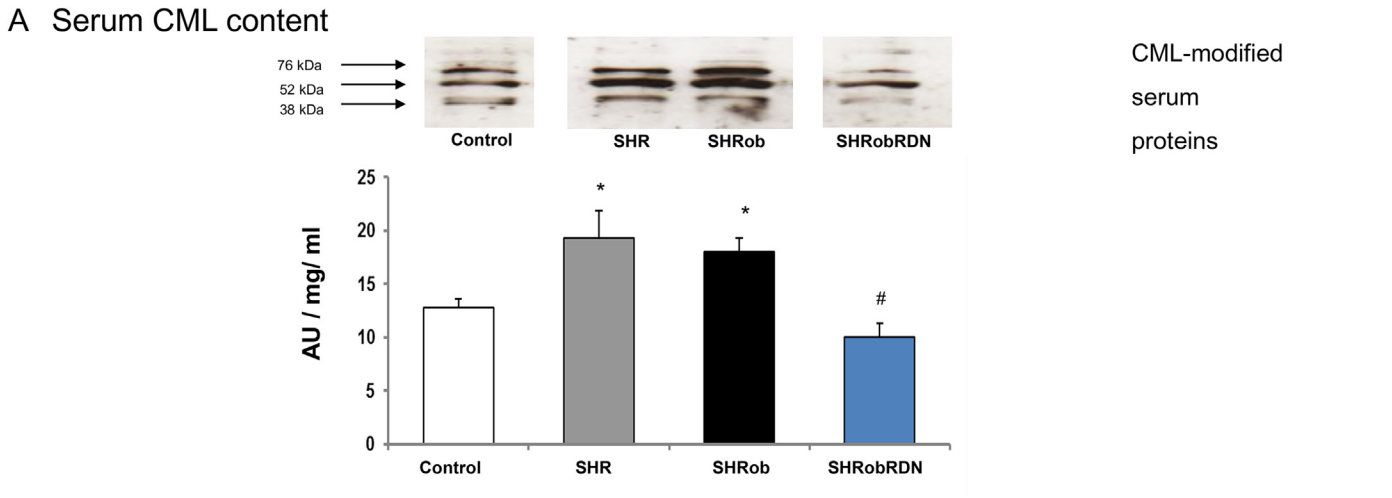

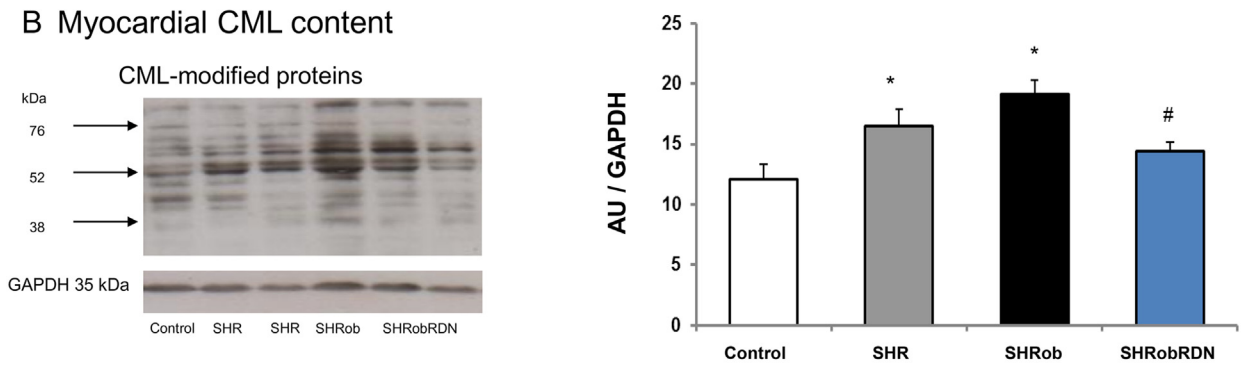

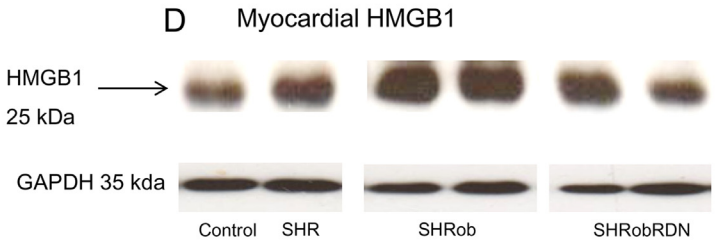

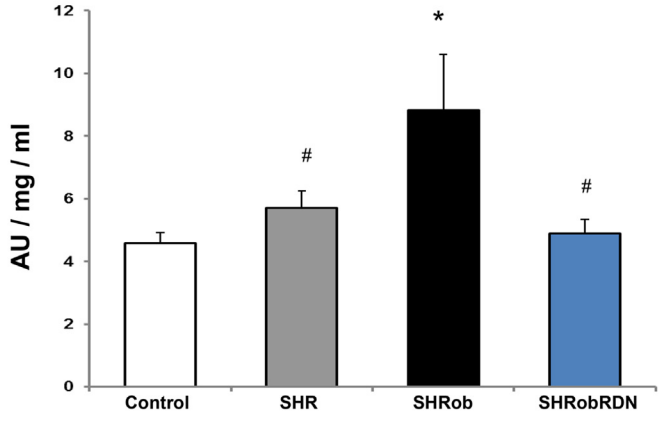

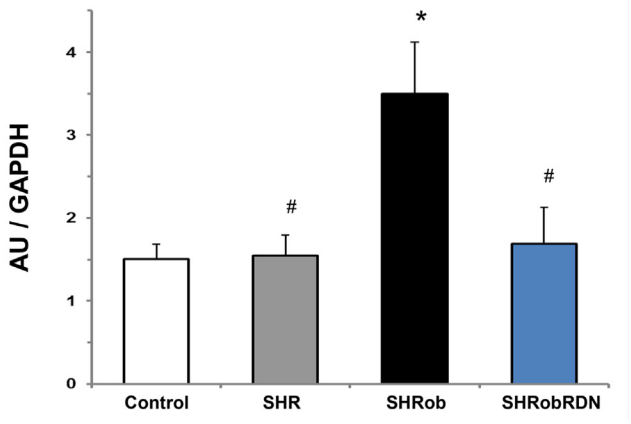

(caption on next page)

Fig. 3. A) Representative Western blot of CML-modified serum proteins (upper panel; images from different parts of the same gel) and quantification of CML by Western blot in serum samples (lower panel) from normotensive controls (n = 5), SHR (n = 6), SHRob (n = 5) and SHRobRDN (n = 5). CML in arbitrary units (AU) normalized to serum protein concentration. The antibody specifically binds to carboxymethyllysine modified proteins and reacts species independently. The antibody recognizes any proteins which have carboxymethyllysine groups. The Western blot shows multiple bands belonging to different proteins. B) Representative Western blot of myocardial CML-modified proteins (left panel) and quantification of CML (right panel) in normotensive controls (n = 5), SHR (n = 6), SHRob (n = 5) and SHRobRDN (n = 5). CML in arbitrary units (AU) normalized to GAPDH. C) Representative Western blot (upper panel) and quantification of HMGB1 in serum samples (lower panel) from normotensive controls (n = 5), SHR (n = 6), SHRob (n = 5) and SHRobRDN (n = 5). HMGB1 in serum samples in arbitrary units (AU) normalized to serum protein concentration. D) Representative Western blot (upper panel; images from different parts of the same gel) and quantification of myocardial HMGB1 (lower panel) in homogenates from normotensive controls (n = 5), SHR (n = 6), SHRob (n = 5) and SHRobRDN (n = 5). HMGB1 in arbitrary units (AU) normalized to GAPDH. E) Representative Western blot (upper panel) and quantification of myocardial TNFα (lower panel) in homogenates from normotensive controls (n = 5), SHR (n = 6), SHRob (n = 5) and SHRobRDN (n = 5). TNFα in arbitrary units (AU) normalized to GAPDH. F) Representative Western blot (upper panel; images from different parts of the same gel) and quantification of myocardial IL-6 (lower panel) in homogenates from normotensive controls (n = 5), SHR (n = 6), SHRob (n = 5) and SHRobRDN (n = 5). IL-6 in arbitrary units (AU) normalized to GAPDH. *p < .05 versus Control; #p < .05 versus SHRob; §p < .05 versus SHR.

+SHRobRDN).

Assessment of the splice variant esRAGE (endogenous secretory RAGE) in both serum (Supplemental Fig. 4A) and myocardial samples (Supplemental Fig. 4B) showed no significant regulation after RDN, although there was a slight but significant increase in myocardial esRAGE in SHRob versus SHR (Table 2; Supplemental Fig. 4B; 0.23 ± 0.01 AU/GAPDH in SHRob versus 0.18 ± 0.01 in SHR, p = .031). Serum esRAGE showed no significant regulation between the groups (Table 2; Supplemental Fig. 4A) and in-vitro cellular esRAGE secretion could not be influenced by isoproterenol stimulation (Supplemental Fig. 4C–D).

3.5. Renal denervation restores RAGE cleaving active ADAM-10

RAGE-cleaving/sRAGE-shedding protease ADAM-10 showed a significant reduction of the active form in SHRob versus SHR (Table 2; Fig. 2F; 12.7 ± 2.8 AU/mg/ml in SHRob, p = .015 versus SHR). Renal denervation restores serum ADAM-10 activity (31.83 ± 5.62 AU/mg/ml in SHRobRDN, p = .028 versus SHRob).

Correspondingly, myocardial ADAM-10 showed decreased activity in SHR (Table 2; Fig. 2G; 8.71 ± 0.64 AU/GAPDH in SHR versus 13.06 ± 0.97 in controls, p = .015) and in SHRob (3.97 ± 0.48 AU/GAPDH, p = .005 versus SHR) and was increased after RDN (9.08 ± 1.24 AU/GAPDH in SHRobRDN, p = .003 versus SHRob). Myocardial ADAM-10 activity correlated positively with myocardial sRAGE (Supplemental Fig. 5: r = 0.85, p = .003, n = 10 SHRob + SHRobRDN).

3.6. Renal denervation decreases circulating and myocardial RAGE-ligand levels of the AGE carboxymethyllysine (CML)

Western blot analysis demonstrated similar levels of the AGE CML in SHR and SHRob in serum samples (Table 2, Fig. 3A) and myocardial tissue (Table 2, Fig. 3B) as well. Renal denervation resulted in a significant reduction of serum CML generation (Fig. 3A; 10 ± 1.3 AU/mg/ml in SHRobRDN versus 18 ± 1.4 AU/mg/ml in SHRob, p = .001) reaching similar CML levels as in normotensive controls (12.7 ± 0.9 AU/mg/ml in controls). The observed changes in serum CML were paralleled by corresponding changes in myocardial CML content (Fig. 3B; 14.4 ± 0.8 AU/GAPDH in SHRobRDN versus 19.2 ± 1.2 AU/GAPDH in SHRob, p = .017). There was a positive correlation between serum CML and myocardial interstitial fibrosis (Supplemental Fig. 6; r = 0.76, p = .04).

3.7. Renal denervation decreases circulating and myocardial RAGE-ligand levels of high-mobility-group-box-1 protein (HMGB1)

Serum HMGB1 levels were significantly higher in SHRob as compared to SHR and normotensive controls (Table 2; Fig. 3C; 8.8 ± 1.8 AU/mg/ml in SHRob versus 5.7 ± 0.5 AU/mg/ml in SHR and 4.6 ± 0.3 AU/mg/ml in controls; p = .035 for SHRob versus SHR). RDN treatment resulted in a significant reduction of HMGB1 serum levels (Fig. 3C; 4.9 ± 0.5 AU/mg/ml in SHRobRDN versus 8.8 ± 1.8 AU/mg/ml in SHRob, p = .026).

SHRob further demonstrated significantly increased myocardial HMGB1 levels as compared to lean SHR and controls (Table 2; Fig. 3D; 3.5 ± 0.6 AU/GAPDH in SHRob versus 1.5 ± 0.3 in SHR and 1.5 ± 0.2 in controls, p < .003 for each comparison). However, again, RDN treatment normalized myocardial HMGB1 protein levels (Fig. 3D; 1.7 ± 0.4 AU/GAPDH in SHRobRDN, p = .022 versus SHRob), achieving similar levels as in lean SHR (1.5 ± 0.3 AU/GAPDH) and normotensive controls alone (1.5 ± 0.2 AU/GAPDH). There was a significant positive correlation between myocardial HMGB1 levels and serum HMGB1 levels in SHRob and SHRobRDN (Supplemental Fig. 7A; r = 0.65; p = .04; n = 10), and between myocardial HMGB1 content and serum CML (Supplemental Fig. 7B; r = 0.7; p = .04). Myocardial HMGB1 also correlated with myocardial RAGE expression (Supplemental Fig. 7C; r = 0.85, p = .003).

3.8. Renal denervation decreases pro-inflammatory cytokines

Western blot analysis of Tumor Necrosis Factor α (TNFα) expression showed a numerical decrease in SHRob versus controls and SHR without statistical significance and without significant regulation after RDN (Table 2; Fig. 3E). Myocardial Interleukine-6 (IL-6) protein content was similar between controls, SHR and SHRob (Table 2, Fig. 3F) and was significantly decreased after RDN (0.59 ± 0.12 AU/GAPDH in SHRobRDN versus 1.34 ± 0.13 in SHRob, p = .001).

3.9. In-vitro-ß-adrenergic stimulation of rat splenocytes decreases sRAGE secretion and increases RAGE expression

Repeated in vitro stimulation (every 24 h) of splenocytes with isoproterenol significantly increased RAGE mRNA expression (Fig. 4A; 91% increase) and membraneous RAGE protein content (Fig. 4B; > 3fold increase). Simultaneously, isoproterenol treatment decreased sRAGE secretion into the cell culture medium (−50%) in a time dependent manner (Fig. 4C), reaching statistical significance after 72 h. Stimulated splenocytes showed no increased apoptosis rate under isoproterenol stimulation as assessed by immunoblot analysis of BAX/BCL-2 in cellular homogenates (not shown).

To differentiate ß-adrenergic receptor subtype-dependent signalling, we also assessed RAGE/sRAGE expression after isoproterenol stimulation in the presence of ß-adrenergic receptor antagonists with differing selectivity: CGP 201712A (ß1-selective) or ICI118.551 (ß2-selective). Isoproterenol induced RAGE-expression was abrogated by ß1-adrenergic receptor blockade with CGP, but not by the ß2-adrenergic receptor blocker ICI (Fig. 4A and B). Contrary to this, sRAGE secretion into the cell culture medium was restored after ß2-adrenergic receptor blockage, but not with ß1-adrenergic receptor blockage (Fig. 4C).

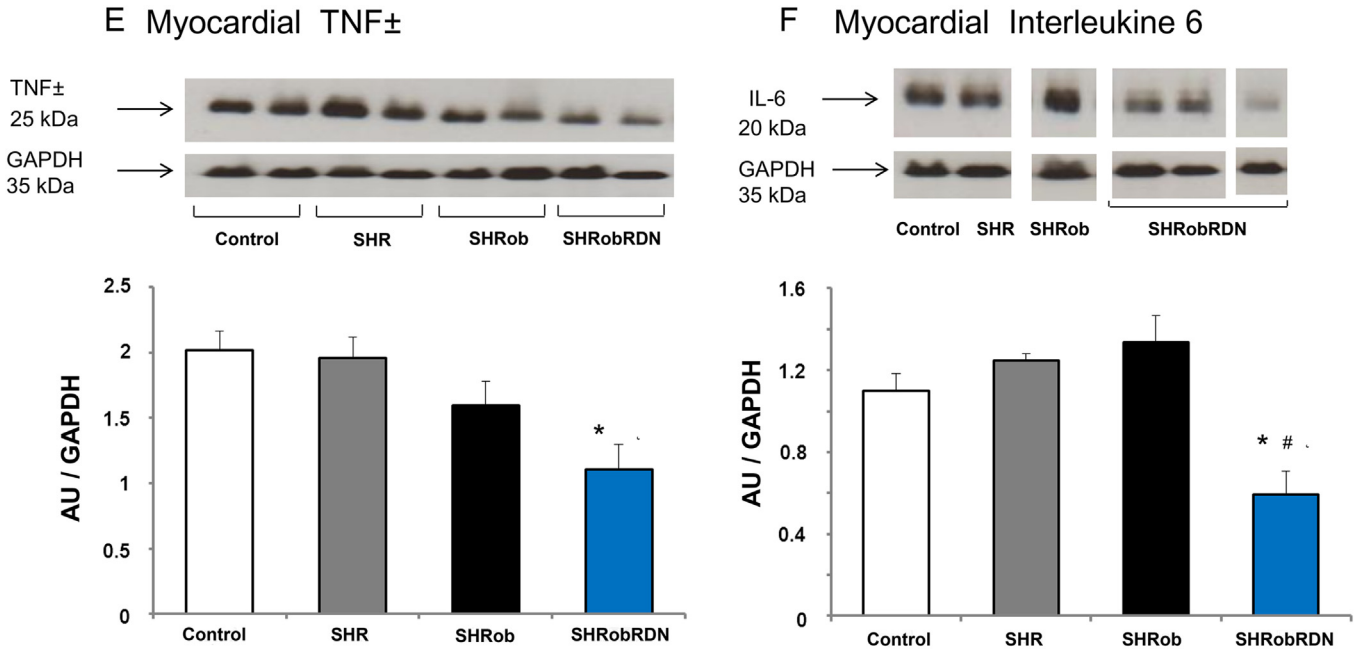

Fig. 3. (*continued*)

3.10. In-vitro-ß-adrenergic stimulation of rat cardiac fibroblasts decreases sRAGE secretion

Neither RAGE mRNA nor membraneous RAGE protein expression were significantly increased in primary rat cardiac fibroblasts after 72 h of isoproterenol treatment (Fig. 4D and E). However, similar to the observed effects in splenocytes, repeated in vitro stimulation (every 24 h) of fibroblasts with isoproterenol decreased sRAGE secretion into the cell culture medium in a time dependent manner (Fig. 4F; −49% decrease after 72 h). Cell vitality in stimulated fibroblast cultures was similar to control.

Again, to better differentiate ß-adrenergic receptor subtype-dependent signalling, cells were co-treated with ß-adrenergic receptor antagonists, and ß2-adrenergic receptor blockage with ICI118.551 prevented the reduction in sRAGE secretion seen with isoproterenol treatment, while ß1-adrenergic receptor blockage had no effect (Fig. 4F).

3.11. In-vitro-ß-adrenergic stimulation of rat splenocytes and rat cardiac fibroblasts decreases sRAGE shedding active ADAM-10

We assessed active ADAM-10 protein levels in supernatants of primary rat cardiac fibroblasts and splenocytes after 72 h of isoproterenol treatment (Fig. 4G–H): active ADAM-10 protein was significantly decreased after isoproterenol treatment (Fig. 4G; −46% decrease in rat splenocytes versus control, and − 72% decrease in cardiac fibroblasts versus control). Co-treatment with ß-adrenergic receptor antagonists showed that ß2-adrenergic receptor blockage with ICI118.551 restored ADAM-10 activity under isoproterenol treatment in both splenocytes and cardiac fibroblasts (Fig. 4G–H).

4. Discussion

Our study characterizes the relationship between sympathoadrenergic activation and RAGE/sRAGE balance in vivo and in vitro. We report favourable effects of sympathetic modulation by renal denervation on serum and myocardial sRAGE/RAGE balance with reduced expression of RAGE ligands like the AGE carboxymethyllysin (CML) and HMGB1 (high-mobility-group-box1 protein) and reduced pro-inflammatory IL-6 in spontaneously hypertensive obese rats, an animal model of hypertension and metabolic syndrome. Furthermore, in vitro ß1-adrenergic stimulation demonstrates direct sympathoadrenergic effects on RAGE expression, as well as ß2-adrenergic stimulation demonstrates direct effects on sRAGE secretion in rat mononuclear cells (splenocytes) and primary cardiac fibroblasts by increasing sRAGE shedding ADAM-10 activity. Taken together, our data indicate a sympathoadrenergic-related and sustained RAGE-mediated pro-inflammatory vicious circle resulting in myocardial remodelling and fibrosis in hypertension and metabolic syndrome.

Metabolic syndrome associated with obesity and hypertension is an increasingly relevant condition. Chronic sympathoadrenergic activation plays a critical role in the development of arterial hypertension [20], which leads to cardiac end-organ damage and heart failure [2, 7, 21]. These pathologies as well as diabetes [1] and obesity [22] have been linked to increased RAGE expression and RAGE activation. A mounting body of evidence suggests that sRAGE is protective by acting as a competitive inhibitor of RAGE [7, 23], not only by neutralizing RAGE-ligands, but also by forming dimers with membrane RAGE and thus blocking RAGE-activation itself [23]. Herein, we show that spontaneously hypertensive rats (SHR), and even more so obese spontaneously hypertensive rats (SHRob) demonstrate a RAGE/sRAGE dysbalance leading to pro-inflammatory and pro-fibrotic processes.

RDN in hypertensive patients has been suggested to induce additional effects beyond blood pressure reduction [14, 21, 24–27]. Here, we provide evidence that suppression of the sympathetic nervous system by RDN has a strong inhibitory effect on the RAGE/sRAGE-ratio under the pathophysiological condition of metabolic syndrome. The observation that ß-adrenergic stimulation resulted in an increase in the RAGE/sRAGE-ratio in vitro in spleen mononuclear cells and cardiac fibroblasts suggests blood pressure-independent immunomodulatory effects after RDN in our animal model for metabolic syndrome. Taken together, our data indicate a sympathoadrenergic- induced and sustained RAGE-mediated pro-inflammatory vicious circle resulting in myocardial remodelling and fibrosis in metabolic syndrome. Our results

deliver a plausible explanation for the observed anti-fibrotic effects of RDN in rats [19], as sRAGE is upregulated after RDN and has been shown to have antifibrotic effects when for example administered in mice with myocardial infarction [26]. In our study, myocardial sRAGE expression showed a strong negative correlation with myocardial fibrosis, potentially representing a sRAGE mediated anti-fibrotic effect. Additionally, RDN also reduced myocardial and blood levels of the AGE CML in RDN-treated rats, which is suggested to be another anti-fibrotic mechanism, as AGEs are known to inhibit collagen degradation [28–31] and are potentially involved in cardiac fibrosis in SHRob and its alteration by RDN.

SHRob rats show a more pronounced diastolic dysfunction compared to their lean littermates SHR. RDN slightly improved systolic and diastolic function in RDN-treated SHRob 3 months after the intervention, as depicted by improved ejection fraction and reduced LVEDP data and reduced fibrosis. Augmentation of systolic and diastolic function has been documented in patients with essential hypertension 6 months after RDN [15]. Nevertheless, our results on RAGE/sRAGE dysbalance in SHRob compared to lean SHR deliver an explanation for the observed add-on effect of metabolic syndrome and obesity in hypertension with regard to aggravation of diastolic dysfunction and systolic dysfunction. Also, myocardial HMGB1 was increased in SHRob as compared to lean SHR and to controls. HMGB1 has been shown by other groups to have negative inotropic effects in isolated contracting cardiac myocytes and might, therefore, worsen cardiac performance [32, 33].

The second RAGE-ligand investigated herein, N-epsilon-carboxymethyl-lysine (CML or carboxymethyllysine), is generated by the non-

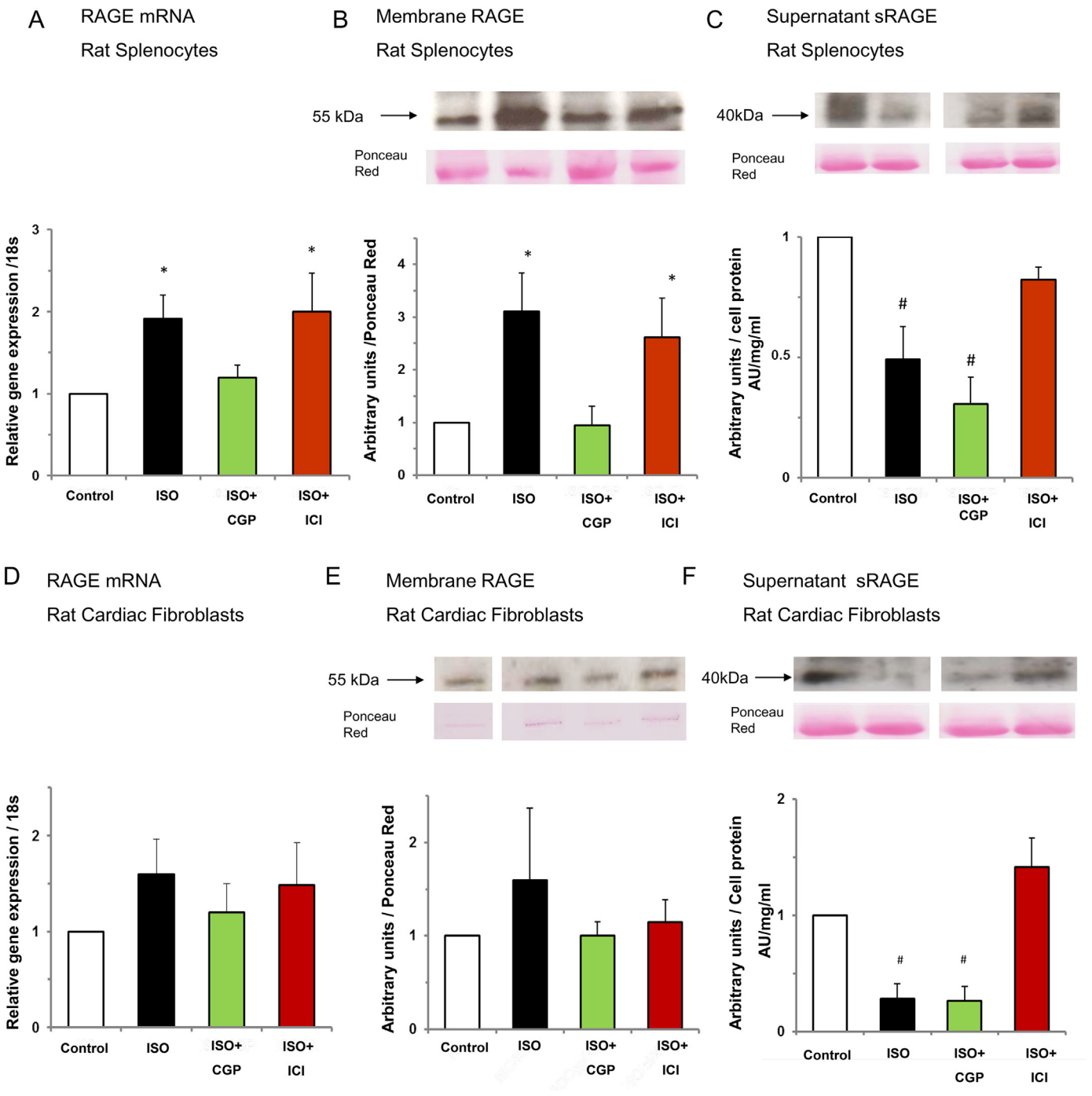

(caption on next page)

Fig. 4. A) Quantification of RAGE mRNA in splenocytes repeatedly stimulated with isoproterenol (ISO) 0.1 μmol/l (n = 4) in the presence or absence of CGP (ß1-selective antagonist; 0.3 μmol/l) or ICI (ß2-selective antagonist; 0.1 μmol/l) for 72 h every 24 h. RAGE mRNA in arbitrary units (AU) with the control sample assigned a value of 1. B) Representative Western blot (upper panel) and quantification of membrane RAGE expression in rat splenocytes (lower panel) repeatedly stimulated with isoproterenol (ISO) 0.1 umol/l (n = 4) in the presence or absence of CGP (ß1-selective antagonist; 0.3 umol/l) or ICI (ß2-selective antagonist; 0.1 umol/l) for 72 h every 24 h. RAGE expression in arbitrary units (AU) with the control sample assigned a value of 1. C) Representative Western blot (upper panel) and quantification of sRAGE secretion in supernatant of splenocytes (lower panel) repeatedly stimulated with isoproterenol (ISO) 0.1 umol/l (n = 4) in the presence or absence of CGP (ß1-selective antagonist; 0.3 umol/l) or ICI (ß2-selective antagonist; 0.1 umol/l) for 72 h every 24 h. sRAGE expression in arbitrary units (AU) with the control sample assigned a value of 1. D) Quantification of RAGE mRNA in rat cardiac fibroblasts repeatedly stimulated with isoproterenol (ISO) 0.1 umol/l (n = 4) in the presence or absence of CGP (ß1-selective antagonist; 0.3 umol/l) or ICI (ß2-selective antagonist; 0.1 umol/l) for 72 h every 24 h. RAGE mRNA in arbitrary units (AU) with the control sample assigned a value of 1. E) Representative Western blot (upper panel) and quantification of membrane RAGE expression in rat cardiac fibroblasts (lower panel) repeatedly stimulated with isoproterenol (ISO) 0.1 umol/l (n = 4) in the presence or absence of CGP (ß1-selective antagonist; 0.3 umol/l) or ICI (ß2-selective antagonist; 0.1 umol/l) for 72 h every 24 h. RAGE expression in arbitrary units (AU) with the control sample assigned a value of 1. F) Representative Western blot (upper panel) and quantification of sRAGE secretion in supernatant of rat cardiac fibroblasts (lower panel) repeatedly stimulated with isoproterenol (ISO) 0.1 umol/l (n = 4) in the presence or absence of CGP (ß1-selective antagonist; 0.3 umol/l) or ICI (ß2-selective antagonist; 0.1 umol/l) for 72 h every 24 h. sRAGE expression in arbitrary units (AU) with the control sample assigned a value of 1. G) Representative Western blot (upper panel; images from different parts of the same gel) and quantification of active ADAM-10 in supernatants of rat splenocytes (lower panel) repeatedly stimulated with isoproterenol (ISO) 0.1 umol/l (n = 4) in the presence or absence of CGP (ß1-selective antagonist; 0.3 umol/l) or ICI (ß2-selective antagonist; 0.1 umol/l) for 72 h every 24 h. Active ADAM-10 protein in arbitrary units (AU) with the control sample assigned a value of 1. H) Representative Western blot (upper panel; images from different parts of the same gel) and quantification of active ADAM-10 in supernatants of rat cardiac fibroblasts (lower panel) repeatedly stimulated with isoproterenol (ISO) 0.1 umol/l (n = 4) in the presence or absence of CGP (ß1-selective antagonist; 0.3 umol/l) or ICI (ß2-selective antagonist; 0.1 umol/l) for 72 h every 24 h. Active ADAM-10 protein in arbitrary units (AU) with the control sample assigned a value of 1. *$p < .05$ versus Control and ISO + CGP; #$p < .05$ versus Control and ISO + ICI. §$p < .05$ versus Control.

enzymatic Schiff base reaction of glucose with proteins, followed by an Amadori rearrangement and oxidation leaving a carboxymethyl group attached to lysine. The levels of CML adducts accumulate over time, indicating both serum glucose levels and oxidative protein damage. Mostly, elevated serum CML modified proteins have been associated with diabetes and complications like diabetic nephropathy, angiopathy and retinopathy. However, CML levels have also been described to be increased in patients and animal models of isolated hypertension [34–36]. Accordingly, we also observed similarly increased CML levels in SHR and SHRob in the absence of diabetes. The exact mechanisms for the increased CML levels remain unclear and warrant future studies.

Recently, soluble fms-like Tyrosine kinase-1 (sFlt-1) has been proposed as a predictive marker for blood pressure reduction after RDN in patients with resistant hypertension [37]. This is particularly intriguing, because AGEs have been shown to be upstream molecules, which trigger ROS-induced sFlt-1 production through a RAGE/NADPH oxidase dependent pathway [38]. Future studies in patients with resistant hypertension are warranted to investigate whether serum levels of AGEs and particularly CML as indicators of long-term oxidative stress could be even more useful biomarkers with predictive value indicating responder and non-responder to sympathomodulation by RDN.

It can only be speculated about the cell types responsible for the observed myocardial and serum sRAGE regulation. Given the cell culture results in primary cardiac fibroblasts, this study strongly implicates the involvement of cardiac fibroblasts in maintaining the myocardial RAGE/sRAGE balance. However, blood mononuclear cells also seem to contribute to the serum sRAGE pool. Furthermore, the induction of membraneous RAGE on mononononuclear cells under β-adrenergic stimulation is especially intriguing, as RAGE is also known to promote cellular adhesion of leukocytes to the vessel wall and migration through the vessel wall into tissue [39]. The effect of sympathoadrenergic hyperactivity affecting RAGE/sRAGE balance is particularly strong in mononuclear cells, by increasing RAGE-expression through ß1-adrenergic receptors on the one hand and decreasing the secretion of sRAGE through ß2-adrenergic receptors signalling on the other hand. This implies a relevant role for the endogenous sympathoadrenergic system in the modulation of the migratory capacity of mononuclear immune cells. In vitro secretion of the RAGE-scavenger sRAGE in cardiac adult fibroblasts also seems to be controlled by the ß2-adrenergic signalling pathway, as seen in mononuclear cells. Thus, sympathetically mediated RAGE-related inflammation is induced by ß1-adrenergic receptor activation and is further augmented by ß2-mediated reduction of sRAGE release.

The antibody used to identify RAGE and total sRAGE did not differentiate between the distinctive soluble RAGE isoforms, namely cRAGE (soluble RAGE formed by protease-mediated cleavage of membraneous full-length RAGE) [8] and esRAGE (endogenous secretory RAGE as a RAGE splice variant lacking the intracellular and transmembrane domain and thus being regularly secreted by cells) [40]. Recent studies have shown that the two isoforms have different relevance as biomarkers in cardiovascular diseases [40]. Differential assessment of serum and myocardial esRAGE in our study showed no significant regulation after RDN, additionally esRAGE secretion in vitro was not influenced by isoproterenol treatment. These observations suggest a RAGE-cleavage mechanism and imply that most of the measured sRAGE in our study is cleaved sRAGE. The in-vitro results point towards a ß2-mediated suppression of RAGE cleavage/sRAGE-shedding by suppression of active ADAM-10, the constitutive sRAGE-producer [8–9]. Additionally, ADAM-10 activity in serum and myocardium was decreased in SHRob and restored after RDN, matching the sRAGE regulation and showing a positive correlation with sRAGE in the heart.

There are some limitations to this study:

We focused in this study on the in vitro effects of ß-adrenergic stimulation. An additional effect of the alpha-adrenergic pathway on RAGE/sRAGE regulation in vivo cannot be excluded. Furthermore, we did not include a group of SHR with RDN because of early re-innervation of the kidney in SHR after the RDN procedure in own pilot experiments (not shown) and the results of previous studies [41, 42]. Consequently, it is difficult to distinguish in vivo between metabolic versus blood pressure effects of RDN. The in-vitro results however are not diminished by this limitation.

5. Conclusions

Sympathoadrenergic activation deteriorates RAGE/sRAGE balance in vivo and in vitro, most likely being involved in cardiovascular end-organ damage. Renal denervation decreases myocardial RAGE/sRAGE-ratio by restoring ADAM-10 activity. These observations might

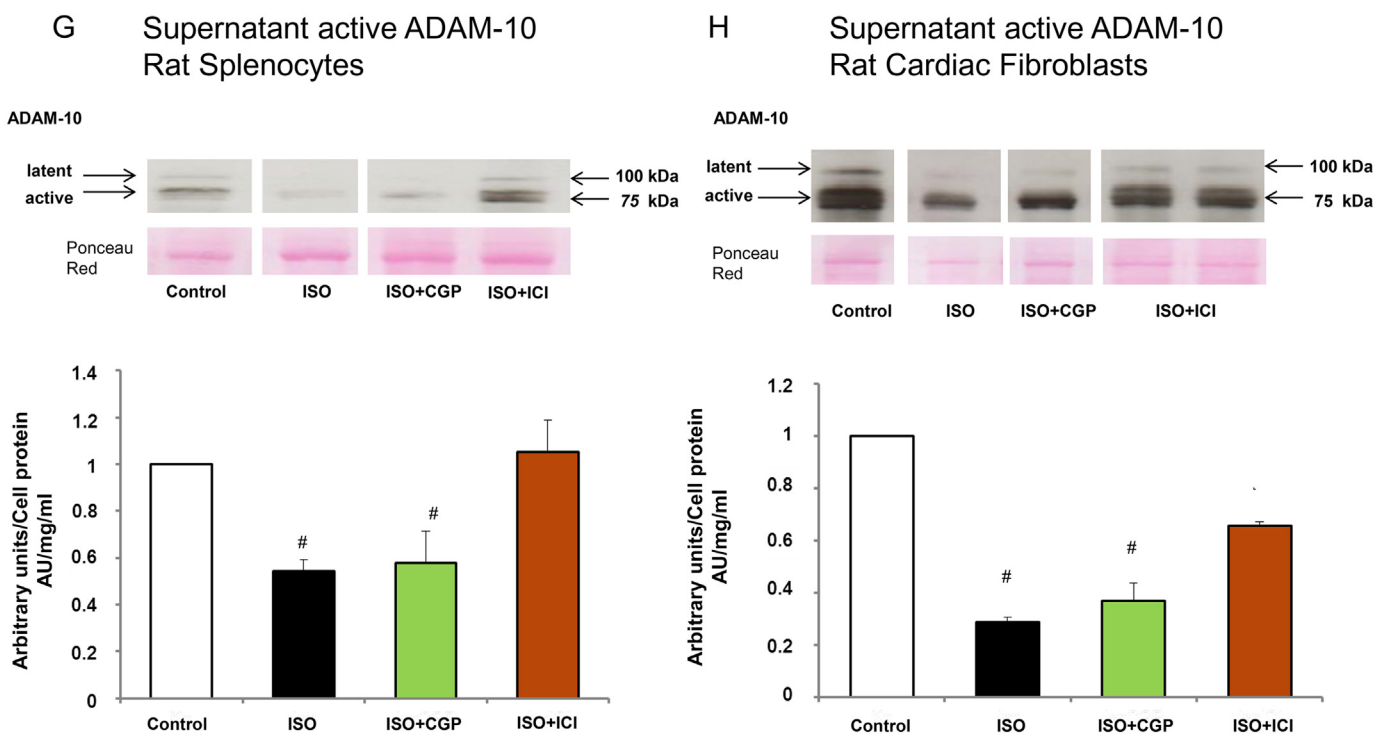

Fig. 4. (*continued*)

therefore be relevant in a wide range of diseases in which the ligand-RAGE axis has been shown to be involved. Prospective studies in patients are needed to confirm this hypothesis.

Funding

This work was supported by HOMFOR 2015/2016, the German Heart Foundation (F/03/15) and the German Research Foundation (SFB/TRR 219 M-02, M-06, S-01, C-08).

Acknowledgements

The authors thank Nina Rebmann, Laura Frisch and Anne Scherer for excellent technical assistance.

Conflict of interest

None declared.

Appendix A. Supplementary data

Supplementary data to this article can be found online at https://doi.org/10.1016/j.yjmcc.2018.08.003.

References

[1] S.F. Yan, R. Ramasamy, Y. Naka, A.M. Schmidt, Glycation, inflammation, and RAGE: a scaffold for the macrovascular complications of diabetes and beyond, Circ. Res. 93 (2003) 1159–1169.
[2] S. Willemsen, J.W. Hartog, D.J. van Veldhuisen, P. van der Meer, J.F. Roze, T. Jaarsma, C. Schalkwijk, I.C. van der Horst, H.L. Hillege, A.A. Voors, The role of advanced glycation end-products and their receptor on outcome in heart failure patients with preserved and reduced ejection fraction, Am. Heart J. 164 (2012) 742–749.
[3] Y. Ihara, K. Egashira, K. Nakano, K. Ohtani, M. Kubo, J. Koga, M. Iwai, M. Horiuchi, Z. Gang, S. Yamagishi, K. Sunagawa, Upregulation of the ligand-RAGE pathway via the angiotensin II type I receptor is essential in the pathogenesis of diabetic atherosclerosis, J. Mol. Cell. Cardiol. 43 (2007) 455–464.
[4] G. Fritz, RAGE: a single receptor fits multiple ligands, Trends Biochem. Sci. 36 (2011) 625–632.
[5] J.N. Tsoporis, S. Izhar, G. Proteau, G. Slaughter, T.G. Parker, S100B-RAGE dependent VEGF secretion by cardiac myocytes induces myofibroblast proliferation, J. Mol. Cell. Cardiol. 52 (2012) 464–473.
[6] Y. Liu, M. Yu, L. Zhang, Q. Cao, Y. Song, Y. Liu, J. Gong, Soluble receptor for advanced glycation end products mitigates vascular dysfunction in spontaneously hypertensive rats, Mol. Cell. Biochem. 419 (2016) 165–176.
[7] S.R. Selejan, J. Pöss, L. Hewera, A. Kazakov, M. Böhm, A. Link, Role of receptor for advanced glycation end products in cardiogenic shock, Crit. Care Med. 40 (2012) 1513–1522.
[8] A. Raucci, S. Cugusi, A. Antonelli, S.M. Barabino, L. Monti, A. Bierhaus, K. Reiss, P. Saftig, M.E. Bianchi, A soluble form of the receptor for advanced glycation endproducts (RAGE) is produced by proteolytic cleavage of the membrane-bound form by the sheddase a disintegrin and metalloprotease 10 (ADAM10), FASEB J. 22 (2008) 3716–3727.
[9] A. Galichet, M. Weibel, C.W. Heizmann, Calcium-regulated intramembrane proteolysis of the RAGE receptor, Biochem. Biophys. Res. Commun. 370 (2008) 1–5.
[10] M. Böhm, F. Mahfoud, C. Ukena, U.C. Hoppe, K. Narkiewicz, M. Negoita, L. Ruilope, M.P. Schlaich, R.E. Schmieder, R. Whitbourn, B. Williams, U. Zeymer, A. Zirlik, G. Mancia, GSR Investigators.First report of the Global SYMPLICITY Registry on the effect of renal artery denervation in patients with uncontrolled hypertension, Hypertension 65 (2015) 766–774.
[11] S. Ewen, F. Mahfoud, D. Linz, J. Pöss, B. Cremers, I. Kindermann, U. Laufs, C. Ukena, M. Böhm, Effects of renal sympathetic denervation on exercise blood pressure, heart rate, and capacity in patients with resistant hypertension, Hypertension 63 (2014) 839–845.
[12] S. Ewen, C. Ukena, D. Linz, I. Kindermann, B. Cremers, U. Laufs, S. Wagenpfeil, R.E. Schmieder, M. Böhm, F. Mahfoud, Reduced effect of percutaneous renal denervation on blood pressure in patients with isolated systolic hypertension, Hypertension 65 (2015) 193–199.
[13] F. Mahfoud, M. Schlaich, I. Kindermann, C. Ukena, B. Cremers, M.C. Brandt, U.C. Hoppe, O. Vonend, L.C. Rump, P.A. Sobotka, H. Krum, M. Esler, M. Böhm, Effect of renal sympathetic denervation on glucose metabolism in patients with resistant hypertension: a pilot study, Circulation 123 (2011) 1940–1946.
[14] M. Böhm, S. Ewen, I. Kindermann, D. Linz, C. Ukena, F. Mahfoud, Renal denervation and heart failure, Eur. J. Heart Fail. 16 (2014) 608–613.
[15] S.H. Schirmer, M.M. Sayed, J.C. Reil, C. Ukena, D. Linz, M. Kindermann, U. Laufs, F. Mahfoud, M. Böhm, Improvements in left ventricular hypertrophy and diastolic function following renal denervation: effects beyond blood pressure and heart rate reduction, J. Am. Coll. Cardiol. 63 (2014) 1916–1923.
[16] D. Linz, A. van Hunnik, M. Hohl, F. Mahfoud, M. Wolf, H.R. Neuberger, B. Casadei, S.N. Reilly, S. Verheule, M. Böhm, U. Schotten, Catheter-based renal denervation reduces atrial nerve sprouting and complexity of atrial fibrillation in goats, Circ. Arrhythm. Electrophysiol. 8 (2015) 466–474.
[17] P. Ernsberger, R.J. Koletsky, J.E. Friedman, Molecular pathology in the obese spontaneous hypertensive Koletsky rat: a model of syndrome X, Ann. N. Y. Acad. Sci. 892 (1999) 272–288.
[18] D. Linz, M. Hohl, F. Mahfoud, J.C. Reil, W. Linz, T. Hübschle, H.P. Juretschke, C. Neumann-Häflin, H. Rütten, M. Böhm, Cardiac remodeling and myocardial

dysfunction in obese spontaneously hypertensive rats, J. Transl. Med. 10 (2012) 187.
[19] D. Linz, M. Hohl, J. Schütze, F. Mahfoud, T. Speer, B. Linz, T. Hübschle, H.P. Juretschke, R. Dechend, J. Geisel, H. Rütten, M. Böhm, Progression of kidney injury and cardiac remodeling in obese spontaneously hypertensive rats: the role of renal sympathetic innervation, Am. J. Hypertens. 28 (2015) 256–265.
[20] M. Böhm, D. Linz, C. Ukena, M. Esler, F. Mahfoud, Renal denervation for the treatment of cardiovascular high risk-hypertension or beyond? Circ. Res. 115 (2014) 400–409.
[21] P.A. Sobotka, F. Mahfoud, M.P. Schlaich, U.C. Hoppe, M. Böhm, H. Krum, Sympatho-renal axis in chronic disease, Clin. Res. Cardiol. 100 (2011) 1049–1057.
[22] K.H. Gaens, C.D. Stehouwer, C.G. Schalkwijk, Advanced glycation endproducts and its receptor for advanced glycation endproducts in obesity, Curr. Opin. Lipidol. 24 (2013) 4–11.
[23] Z. Sárkány, T.P. Ikonen, F. Ferreira-Da-Silva, M.J. Saraiva, D. Svergun, A.M. Damas, Solution structure of the soluble receptor for advanced glycation end products (sRAGE), J. Biol. Chem. 286 (2011) 37525–37534.
[24] C. Ott, F. Mahfoud, A. Schmid, T. Ditting, R. Veelken, S. Ewen, C. Ukena, M. Uder, M. Böhm, R.E. Schmieder, Improvement of albuminuria after renal denervation, Int. J. Cardiol. 173 (2014) 311–315.
[25] D. Linz, A. van Hunnik, C. Ukena, S. Ewen, F. Mahfoud, S.H. Schirmer, M. Lenski, H.R. Neuberger, U. Schotten, M. Böhm, Renal denervation: effects on atrial electrophysiology and arrhythmias, Clin. Res. Cardiol. 103 (2014) 765–774.
[26] A. Aleshin, R. Ananthakrishnan, Q. Li, R. Rosario, Y. Lu, W. Qu, F. Song, S. Bakr, M. Szabolcs, V. D'Agati, R. Liu, S. Homma, A.M. Schmidt, S.F. Yan, Ramasamy R.RAGE modulates myocardial injury consequent to LAD infarction via impact on JNK and STAT signalling in a murine model, Am. J. Physiol. Heart Circ. Physiol. 294 (2008) H1823–H1832.
[27] L. Donazzan, F. Mahfoud, S. Ewen, C. Ukena, B. Cremers, C.M. Kirsch, D. Hellwig, T. Eweiwi, S. Ezziddin, M. Esler, M. Böhm, Effects of catheter-based renal denervation on cardiac sympathetic activity and innervation in patients with resistant hypertension, Clin. Res. Cardiol. 105 (2016) 304–371.
[28] D.J. Campbell, J.B. Somaratne, A.J. Jenkins, D.L. Prior, M. Yii, J.F. Kenny, A.E. Newcomb, C.G. Schalkwijk, M.J. Black, D.J. Kelly, Diastolic dysfunction of aging is independent of myocardial structure but associated with plasma advanced glycation end-product levels, PLoS One 7 (2012) e49813.
[29] I. Russo, N.G. Frangogiannis, Diabetes-associated cardiac fibrosis: cellular effectors, molecular mechanisms and therapeutic opportunities, J. Mol. Cell. Cardiol. 90 (2016) 84–93.
[30] M.P. Begieneman, L. Rijvers, B. Kubat, W.J. Paulus, A.B. Vonk, A.C. van Rossum, C.G. Schalkwijk, W. Stooker, H.W. Niessen, P.A. Krijnen, Atrial fibrillation coincides with the advanced glycation end product N(ε)-(carboxymethyl)lysine in the atrium, Am. J. Pathol. 185 (2015) 2096–2104.
[31] J. Zhao, R. Randive, J.A. Stewart, Molecular mechanisms of AGE/RAGE-mediated fibrosis in the diabetic heart, World J. Diabetes 5 (2014) 860–867.
[32] H.P. Tzeng, J. Fan, J.G. Vallejo, J.W. Dong, X. Chen, S.R. Houser, D.L. Mann, Negative inotropic effects of high-mobility group box 1 protein in isolated contracting cardiac myocytes, Am. J. Physiol. Heart Circ. Physiol. 294 (2008) H1490–H1496.
[33] W. Liu, J. Deng, J. Xu, H. Wang, M. Yuan, N. Liu, Y. Jiang, J. Liu, High-mobility group box 1 (HMGB1) downregulates cardiac transient outward potassium current (Ito) through downregulation of Kv4.2 and Kv4.3 channel transcripts and proteins, J. Mol. Cell. Cardiol. 49 (2010) 438–448.
[34] S. Gawandi, S. Gangawane, A. Chakrabarti, S. Kedare, K. Bantwal, V. Wadhe, A. Kulkarni, S. Kulkarni, M.G.R. Rajan, A Study of Microalbuminuria (MAU) and Advanced Glycation End Products (AGEs) Levels in Diabetic and Hypertensive Subjects, Indian J. Clin. Biochem. 33 (2018) 81–85.
[35] M. Baumann, C. Stehouwer, J. Scheijen, U. Heemann, H. Struijker Boudier, C. Schalkwijk, N epsilon-(carboxymethyl)lysine during the early development of hypertension, Ann. N. Y. Acad. Sci. 1126 (2008) 201–204.
[36] X. Wang, K. Desai, J.T. Clausen, L. Wu, Increased methylglyoxal and advanced glycation end products in kidney from spontaneously hypertensive rats, Kidney Int. 66 (2004) 2315–2321.
[37] O. Dörr, C. Liebetrau, H. Möllmann, L. Gaede, C. Troidl, J. Rixe, C. Hamm, H. Nef, Soluble fms-like tyrosine kinase-1 and endothelial adhesion molecules (intercellular cell adhesion molecule-1 and vascular cell adhesion molecule-1) as predictive markers for blood pressure reduction after renal sympathetic denervation, Hypertension 63 (2014) 984–990.
[38] Q.T. Huang, M. Zhang, M. Zhong, Y.H. Yu, W.Z. Liang, L.L. Hang, Y.F. Gao, L.P. Huang, Z.J. Wang, Advanced glycation end products as an upstream molecule triggers ROS-induced sFlt-1 production in extravillous trophoblasts: a novel bridge between oxidative stress and preeclampsia, Placenta 34 (2013) 1177–1182.
[39] T. Chavakis, A. Bierhaus, N. Al-Fakhri, D. Schneider, S. Witte, T. Linn, M. Nagashima, J. Morser, B. Arnold, K.T. Preissner, P.P. Nawroth, The pattern recognition receptor (RAGE) is a counterreceptor for leukocyte integrins: a novel pathway for inflammatory cell recruitment, J. Exp. Med. 198 (2003) 1507–1515.
[40] S. Moriya, M. Yamazaki, H. Murakami, K. Maruyama, S. Uchiyama, Two soluble isoforms of receptors for advanced glycation end products (RAGE) in carotid atherosclerosis: the difference of soluble and endogenous secretory RAGE, J. Stroke Cerebrovasc. Dis. 23 (2014) 2540–2546.
[41] G.D. Fink, J.T. Phelps, Can we predict the blood pressure response to renal denervation? Auton. Neurosci. 204 (2017) 112–118.
[42] S.R. Winternitz, R.E. Katholi, S. Oparil, Role of the renal sympathetic nerves in the development and maintenance of hypertension in the spontaneously hypertensive rat, J. Clin. Invest. 66 (1980) 971–978.